Influence of Structure Size and Geometry on Wetting Behavior of PMMA Surfaces Imprinted with Laser-Textured Stamps

Felix Bouchard[1], Wei Wang[1], Marcos Soldera[1] and Andrés F. Lasagni[*1,2]

[1] *Institut für Fertigungstechnik, Technische Universität Dresden, George-Baehr-Str. 3c, 01069 Dresden, Germany*
[2] *Fraunhofer-Institut für Werkstoff- und Strahltechnik (IWS), Winterbergstraße 28, 01277 Dresden, Germany*
[*]*Corresponding author's e-mail: felix.bouchard1@tu-dresden.de*

In this study, the wetting behavior of micro-structured poly(methyl methacrylate) (PMMA) surfaces produced by plate-to-plate hot embossing is investigated. The embossing tools used consist of stainless steel plates, which were previously processed by different laser methods, namely Direct Laser Engraving (DLE), Direct Laser Writing (DLW) and Direct Laser Interference Patterning (DLIP). Various textures with spatial periods in the range 1.7 to 900 µm and structure depths between 0.1 and 50 µm were produced and successfully transferred to 175 µm thick PMMA films at an embossing temperature of 130°C. In all cases, the imprints displayed the negative of the stamp textures with a difference between the stamp depth and imprint height between 6 and 16 %. The wetting behavior of the PMMA surfaces was investigated by measuring the static contact angle of distilled water as well as linseed oil. The measurements revealed an increase in the water contact angle from 79° up to 142° on the DLE-based surfaces, whereas for linseed oil, a decrease from 20° to 5° was observed for the same sample. In addition, the PMMA foils were also treated with a hydrophobizing agent in order to modify the surface chemistry. The measurements revealed no change in the water contact angle, whereas for linseed oil, contact angles up to 142° on a hierarchical surface were reached.

DOI: 10.2961/jlmn.2022.02.2006
Keywords: hot embossing, hierarchical structure, poly(methyl methacrylate), direct laser interference patterning, direct laser writing, laser engraving, wetting behavior.

1. Introduction

Flora and fauna provide numerous examples of hierarchical surface textures with outstanding technical properties such as the self-cleaning behavior of the lotus leaf or the super-oleophobic skin of the spring tail [1,2]. The imitation and transfer of the easy-to-clean property of the lotus leaf, for example, to technical surfaces has been the subject of numerous studies by engineers in recent decades [3,4]. Polymer materials are of particular interest due to their inexpensive production and widespread utilization. Technical parts made of poly(methyl methacrylate) (PMMA) have become a relevant material due to its low weight, high chemical stability and high transparency. In particular, optical applications of PMMA include displays, architectural glass or protective cover for light sources. In addition, the response of PMMA surfaces in contact with liquids can be tuned to achieve advanced applications, such as easy-to-clean or anti-biofilm effects.

The wetting behavior can be specifically modified by chemical coatings [5–7], plasma treatment [8–10] or surface laser based structuring [11–13]. Also combined methods including surface textures and coatings with super-amphiphobic and amphiphilic behavior have already been developed [14]. However, these processes often require the use of environmentally harmful substances or are not suitable for mass production. Indirect surface structuring by hot embossing is an alternative method, which produces no hazardous agents and is compatible with industrial processes.

Hot embossing is a fabrication technique that can be used to replicate micro-textures form a mold to a polymer. In order to achieve high replication quality, temperature and holding time are the key parameters. [15,16]. As embossing tools (molds), metals are used due to their durability and low costs. Fabrication of micro-textured molds can be done with CNC micro-milling [17], lithography [18], etching [19] and also with laser based techniques.

The idea of utilizing laser-based micro-fabrication to texture embossing tools is not new. Choi et al. [11] produced micro-fluidic channels on stainless steel (AISI 304 L) using fs-laser texturing. The channels showed a depth of 10 µm with a width of 75 µm and were embossed on PMMA. Zhu et al. [20] used ultrasonic embossing with ns-laser textured steel and aluminum tools on polyethylene-terephthalate films. Pillar-like micro-textures with a pitch of 80 µm were embossed on PET films and showed an increased water contact angle from 70.7° to 100.4°.

Depending on the laser technique, different structure resolutions are possible. With conventional Direct Laser Writing (DLW), structure resolutions up to 5-30 µm have already been reported [21]. Structures larger than approximately 300 µm are possible to fabricate by Direct Laser Engraving (DLE) [22]. For micro- and nano-structuring with feature sizes smaller than 10 µm, Direct Laser Interference Patterning (DLIP) technique has become an established process in recent years [23]. In DLIP, a single laser beam is split up into

multiple sub-beams that are superimposed on the target surface at a specific angle of incidence Θ. If two sub-beams are used, a line-like intensity distribution is formed in the overlapping area, where the spatial period Λ depends on the laser wavelength λ and the incidence angle. For two beams, the spatial period is given by [24]:

$$\Lambda = \frac{\lambda}{2 \cdot \sin\frac{\theta}{2}} \quad (1)$$

When four beams are used, a periodic dot-shaped intensity distribution is formed with a spatial period of [25]:

$$\Lambda = \frac{\lambda}{\sqrt{2} \cdot \sin\frac{\theta}{2}} \quad (2)$$

Even smaller textures can be obtained by applying ultrashort laser pulses (in the fs to ps regime) on a material so that the so-called Laser-Induced Periodic Surface Structures can be formed. On metals, these self-assembled nano- or sub-microstructures arise due to the interaction between the surface and plasmonic resonances and can be controlled by adjusting the cumulated fluence, pulse duration and polarization direction, among other factors [26,27]. Yao et al. and Rakabrandt et al. [28,29] reported a successful transfer of LIPSS with periods of 600-700 nm from fs-laser treated steel to polymer sheets via hot embossing.

In this work, laser-structuring techniques, namely DLE, DLW and DLIP are employed for texturing metallic tools for plate-to-plate hot embossing. These tools are used to control the wettability behavior of PMMA foils for polar- and non-polar liquids. Due to the different resolutions that can be achieved with each technique, the structure parameters (shape, depth and period) are varied to determine their influence on the wetting contact angle. Various structure geometries, such as line-like, dot-like but also more exotic shapes as donut-like textures were created. The wetting behavior of imprinted PMMA is determined for each single scaled surface. Finally, structure combinations with two length-scales are produced in order to evaluate the potential to further improve the wetting behavior.

2. Materials and methods

2.1 Materials

For laser structuring treatment, stainless steel plates (1.4301, Designblech GmbH, Germany) with dimensions of 80 mm x 60 mm, a thickness of 0.8 mm and an initial roughness S_q of 15 nm were used. After laser texturing, the plates served as masters for plate-to-plate hot embossing. Imprints were obtained on poly-methyl-methacrylate (PMMA) foils (Evonik Performance Materials, Darmstadt, Germany) with a thickness of 175 µm and a glass transition temperature of 130°C.

2.2 Laser processing methods

Laser structuring of stainless steel plates was performed using two techniques of direct laser structuring, namely Direct Laser Writing (DLW) and Direct Laser Interference Patterning (DLIP). In DLW, the laser is guided over the sample surface using a scanner system. Large areas can be processed with parallel lines, whereas the ablation behavior of the material within the laser spot determines the feature geometry on the surface. Direct Laser Engraving (DLE) is a variation of the DLW technique, where the surface is scanned linewise with parallel lines at a close distance. Each scan represents a layer. Multiple layers can be applied in order to create a 2.5 dimensional surface texture.

In this study, DLW and DLE were performed with a commercial available laser surface texturing station (P600U, GF machining solutions, Switzerland), equipped with an ytterbium fiber laser operating at 1064 nm and an average power output of 30 W. The system operates at frequencies between 2 kHz and 1000 kHz and the pulse duration can be tuned between 4 ns and 200 ns. An integrated galvanometer scanner system, equipped with an F-theta lens, provides an operating speed up to 10 m/s with a laser spot size of 60 µm.

Two-beam direct laser interference patterning (2B-DLIP) was performed using a self-developed DLIP system, equipped with a DLIP-optical head (Fraunhofer IWS, Germany) and a picosecond laser source (Edgewave PX200, Germany) operating at 1064 nm. A detailed description of the system can be found elsewhere [30].

Four-beam direct laser interference patterning (4B-DLIP) was performed using a self-developed system, equipped with a 70 ps solid-state pulsed laser (NeoMos 70ps, NeoLASE GmbH, Hannover, Germany). The system provides a repetition rate of 1-10 kHz at a wavelength of 532 nm with a maximum power output of 7.5 W. Further information of the used system can be found elsewhere [31].

2.3 Hot embossing treatment of PMMA

Hot embossing process was performed using a hydraulic press (Paul-119 Otto Weber GmbH, Germany), providing pressing forces of 100-1000 kN in a temperature range of 40°C to 400°C. To assure a homogeneous pressure distribution, the polymer foils were placed between the metal master and a rubber-like sheet of high-performance silicone (Exact plastic GmbH, Bröckel, Germany) with a thickness of 3 mm. To prevent friction between the metal and the silicone during pressing, a sheet of baking paper was placed between them. To avoid sticking, the metal plates were initially cleaned with ethanol, dried with compressed air and finally spray coated with a non-toxic anti-sticking-agent (Mecasurf, Surfactis Technologies, Angres, France).

2.4 Contact angle measurements

Contact angle measurements were performed with deionized water and linseed oil (cold pressed linseed seed oil, Kunella Feinkost GmbH, Cottbus; Germany) using a commercially available droplet shape analyzer (Krüss DSA 100 S, Hamburg, Germany). The analyses were performed using the Young-Laplace fitting method. Before measurements, the PMMA samples were cleaned with a jet of compressed air and rinsed with ethanol. For contact angle measurements with oil, the polymer samples were either directly used or after dip-coating them with a perfluoropolyether compound (Mecasurf, Surfactis Technologies, Angres, France). The coated samples were dried under atmospheric conditions for 5 min followed by a jet of compressed air. Measurements were taken under normal ambient conditions (22 °C, 16 % R.H.). For statistical analysis, the average of five measurements were taken at different positions. Before and between measurements, samples were rinsed with warm water and ethanol before drying with a jet of air again.

2.5 Surface characterization

The morphology of the laser engraved metal masters as well as imprinted polymer foils were measured using confocal microscopy (Sensofar S neox, Sensofar S.A., Spain) with magnification objectives of 20x and 50x. The obtained topographical data were analyzed using SensoMap software (SensoMap "Premium" Version 7, Sensofar 140 S.A.).

3. Results and discussion

In this study, an experimental approach was followed to determine optimal texture combinations of different dimensions using three laser-based methods: DLW, DLE and DLIP. In addition, hierarchical surfaces were producing by combination of these methods obtaining surface textures with different length scales. For each of the mentioned processes, common structure resolutions were chosen based on the technically possible limits for texturing stainless steel. The maximum structure depths were limited to aspect ratios (height to period ratio h/Λ) below 0.4. This value was selected from previous investigations, since higher values can lead to the attachment of the polymer foil to the metallic embossing tool.

3.1 Wetting behavior of PMMA foils with simple structure geometry

In a first set of experiments, periodic structures with a simple geometry were produced using direct laser engraving (DLE), direct laser writing (DLW) and direct laser interference patterning (DLIP). For each condition, fields of 10x10 mm² were processed on stainless steel. The steel plates served as master for a plate-to-plate hot embossing process with a temperature of 130°C, a pressure of 1.1 MPa and a holding time of 10 min. These process parameters has been chosen according to previous studies by Wu et al. [32].

The structures on the steel master and the according PMMA imprint can be seen in Figure 1. The DLE-grid like texture, shown in Figure 1a, was produced by scanning the steel surface 40 times in a line-wise movement with a line-to-line distance of 10 µm. One layer of material was removed with each scan, and the scanned areas were thinned with each scan to obtain a 2.5D topography with a triangular profile. The optimum process parameters were determined in preliminary experiments. Therefore, the pulse duration was set to 30 ns with a constant laser fluence of 21.2 J/cm² per pulse. The pulse frequency was 100 kHz and the feeding rate 1000 mm/s. A detailed description of this established DLE strategy and the influence of different process parameters was already given by Nikolidakis et al. [33].

As a result, plateau like areas were created on the metal, separated by grooves with depths of 54 µm and widths of 90 µm. The top area of each plateau remained untreated with the initial roughness of 15 nm and was also surrounded by formations of molten material with a height of up to 8 µm next to the grooves. The embossed PMMA surface showed the inverted morphology with grid like walls with heights of 50 µm and a width of 5 µm on top. The areas between the walls remained flat, surrounded by 8 µm deep grooves.

The DLW dot-like pattern, depicted in Figure 1b, was processed by applying 30 pulses per spot at a frequency of 130 kHz and a laser fluence of 11.8 J/cm² following a hexagonal arrangement with a periodic distance of 80 µm. The pulse duration was 30 ns. As it can be seen, holes with depths of 17 µm surrounded by molten material were created on the master. The according imprint showed pillar-like formations where the polymer flowed into the cavities of the metal master during the hot embossing. The average height of the pillars was 6.8 µm with a diameter of 30 µm on top.

The DLIP line-like structure, shown in Figure 1c, was processed with a two beam ps-laser system with a spot diameter of 80 µm at a frequency of 10 kHz. The sub-beams were focused on the metal surface with an angle of incidence of 14.2° resulting in a spatial period of 4.3 µm. The overlap between single pulses (in the direction along the interference lines) was set to 90 % with a line-to-line spacing of 100 µm. As result, periodic line-like textures with an average depth of 483 nm were processed on the master. The PMMA imprint showed a similar profile geometry with heights of 425 nm in average.

The above mentioned structures were fabricated with varying depths on steel and replicated on PMMA with constant stamping parameters.

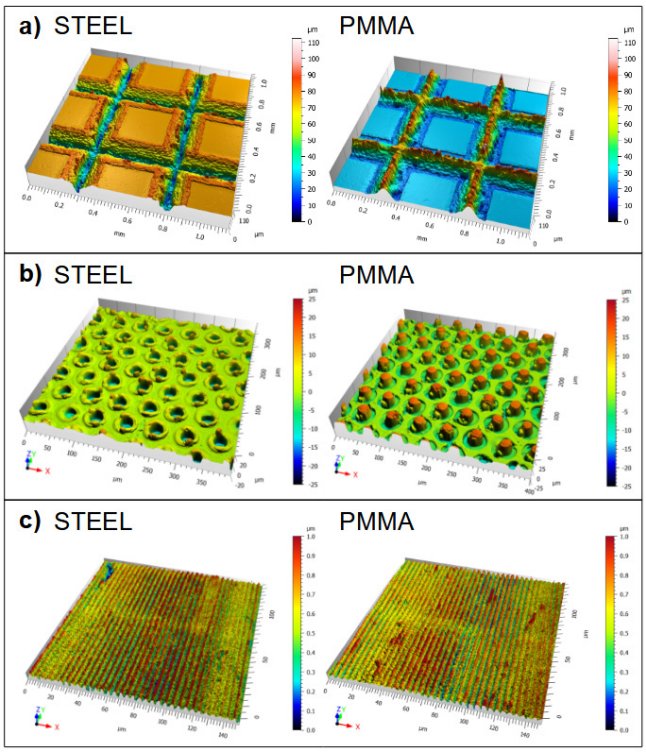

Fig. 1 Laser processed surfaces on stainless steel master and corresponding imprints on PMMA foil for (a) grid like DLE-structure with period of 500 µm, (b) DLW dot-like structure with period of 80 µm and (c) DLIP line-like texture with period 4.3 µm. Depicted areas are (a) 1.15 mm x 1.15 mm, (b) 350 µm x 350 µm and (c) 80 µm x 80 µm.

Figure 2 shows the measured depths in the master (full markers) and the corresponding heights on the PMMA imprint (empty markers) for DLE, DLW and DLIP structures. For DLE (Figure 2a), periods of 300 – 900 µm were processed and the depth was controlled by adjusting the number of scanning cycles between 10 – 40. It is clear to see, that the engraved depth increased for smaller periods. Structures with a period of 900 µm, for instance, showed a depth of 47 µm in 40 scans. With a period of 300 µm, a depth of 64

µm was reached. Considering that all laser parameters remained fixed for this set of experiments, the decrease of the structure depth as the spatial period increased can be ascribed to the followed structuring strategy, whereby the shorter periods were achieved at higher number of laser passes than the longer ones. Therefore, for patterning the shorter periods more cumulated fluence was applied and thus more molten and/or ablated material was expected [34-37].

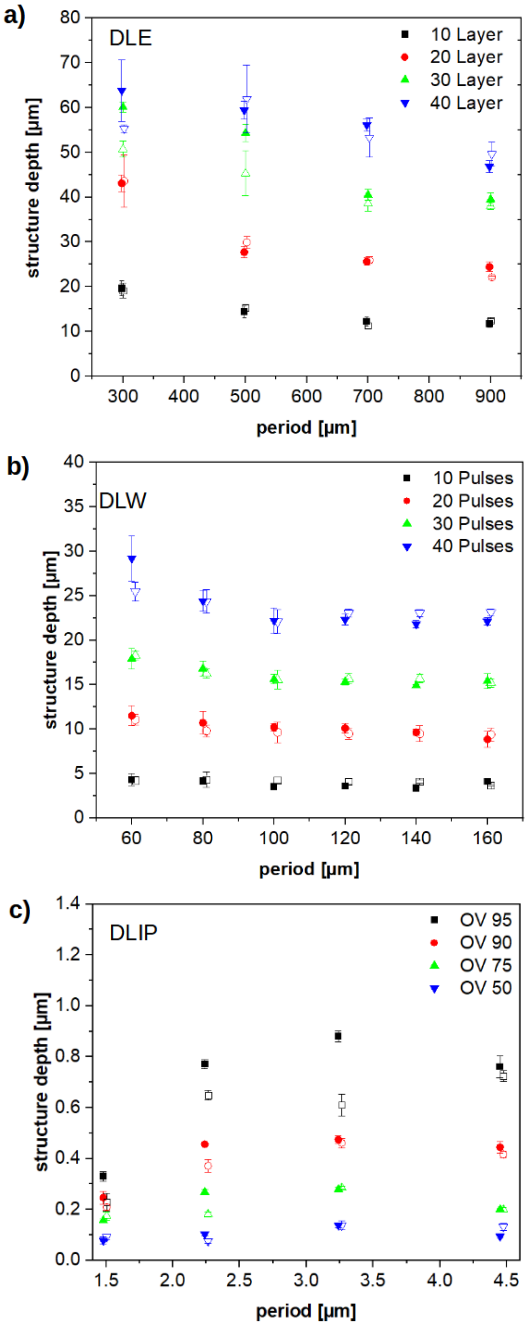

Fig. 2 Structure depth on stainless steel master plates and related heights on imprinted PMMA (empty symbols) for structure periods produced with (a) DLE, (b) DLW and (c) DLIP.

For DLW (Figure 2b), the period (distance between the dots) was varied between 60 µm and 160 µm and the number of applied pulses was between 10 and 40 pulses. The depth on the master increases with the number of applied pulses up to 29 µm for 40 pulses. On the corresponding imprint, a height of only 25 µm was determined, indicating insufficient filling of the cavities in the master. For all the DLW experiments, the heights and depths of the structures on the master and imprint were comparable.

For the DLIP method (Figure 2c), line-like structures with periods between 1.5 and 4.3 µm were produced with varying pulse-to-pulse overlaps from 50% up to 95%. The deepest structures were 773 nm with a period of 3.4 µm. On the corresponding imprint, a depth of 687 nm was measured. In general, better replication was observed for smaller periods and lower depths.

From this set of experiment, it can be concluded that the used embossing parameters are satisfactory to reproduce the patterns of the textured embossing tools.

After that, preliminary contact angle (CA) measurements were performed to evaluate the effect of structure depth on the wetting behavior. During the first imprints, it was observed that dust and other micro-particles were transferred from the laser textured areas to the polymer. To avoid a contamination, contact angle measurements of embossed surfaces were performed after the 10th imprint.

Exemplary results for water and linseed oil are presented in Figure 3a and b, respectively. For the water CA measurements, the textured polymer foils exhibited angles between 95° and 114°. In all cases, the oil CA of the textured PMMA foils was below 21° and for the DLIP structures, a nearly super-oleophilic character was observed with CA lower than 10°.

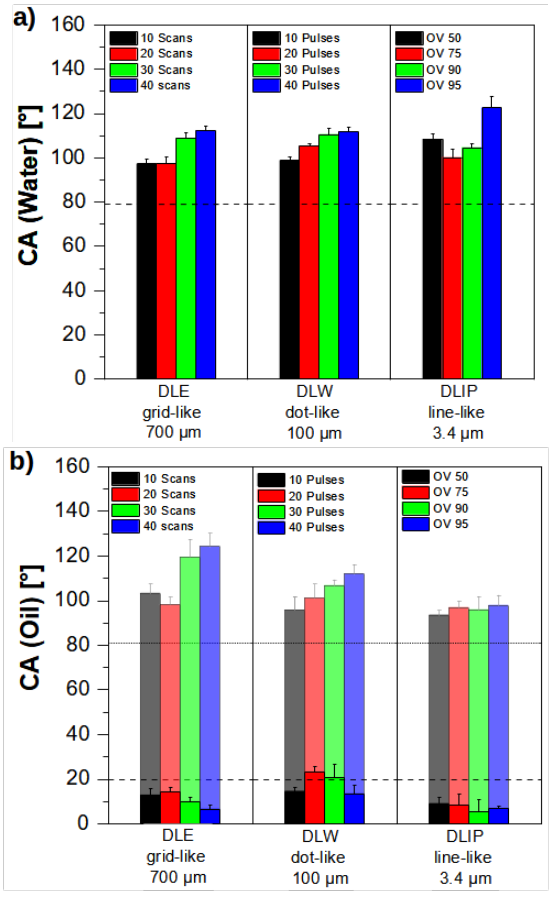

Fig. 3 Static contact angles for (a) deionized water and (b) linseed oil on micro-structured PMMA with simple feature geometries. References (dashed lines) were 79° for water and 20° for linseed oil. For oil, structures were additionally coated with Mecasurf (shallow bars). When coated, the reference (dotted line) contact angle is 81°.

The wetting behavior of patterned polymer surfaces has already been the subject of numerous studies [38,39]. The Wenzel and Cassie-Baxter models have proved to be simple yet effective approaches for describing the relationship between roughness and contact angle. According to Wenzel's theory, a liquid droplet in contact with the structured surface penetrates the protrusions of the texture, wetting completely the valleys and peaks of the topography. The model suggests that hydrophobic or hydrophilic wetting behavior becomes reinforced by increasing the surface roughness [40]. On the contrary, Cassie-Baxter model assumes that when a rough surface is wetted, air pockets are formed that prevent the liquid from infiltrating into the texture valleys. As a result, the contact angle increases with increasing roughness, independent of the initial contact angle or wetting state [41].

In this study, it can be assumed that the hot stamping process did not modify the surface chemistry of PMMA, and thus all changes in wetting behavior can be attributed to the increase of surface roughness. When wetted with water, all microstructured surfaces showed a change from the initial slightly hydrophilic state with contact angles of 79° to a hydrophobic one characterized by contact angles between 95° and 122°. Thus, a Cassie-Baxter wetting state or a mixed state can be assumed, in which air remains in the cavities of the textured surface. An opposite behavior was observed for the oil wetting experiments. In this case, the microstructured surfaces showed contact angles lower than that of the oleophilic smooth reference surface (20°). It can be thus assumed that a wetting state according to Wenzel's model is present here, in which the oil penetrates and wets the pits and trenches of the surface.

For easy-to-clean applications, surfaces must be both hydrophobic and oleophobic. Since the produced surfaces showed an oleophilic characteristic, the effect of an additional chemical modification with a hydrophobizing agent (Mecasurf) was investigated. MecaSurf is a chemically active perfluoropolyether containing ethoxydifluoromethyl terminal groups that physically interact with the pendant ester groups of polymethylmethacrylate (PMMA) generating attractive electrostatic dipole-dipole induced and London forces. These electrostatic forces favor the adhesion of both non-polar compounds forming an ultrathin layer (<5 nm) [42].

Without the chemical modification, the oil droplets spread within few minutes over the entire structured surface. This effect is shown in Figure 4 (top-right area). In case of the coated structured foils, drops of oil had a relatively large contact angle and retained their shape even after several minutes. The effects of the coating are also shown in Figure 4 (bottom-left: reference surface, bottom-right: micro-textured areas).

When coated with Mecasurf, the oil CA on the imprinted foils varied between 93° and 124° depending on the used technology and chosen parameters, as shown in Figure 3b. The highest value was obtained for the DLE texture processed with 40 scanning cycles. For water (not shown), no visible difference between the coated and non-coated surfaces was observed and in consequence, only the water CA without Mecasurf coatings are reported in this study.

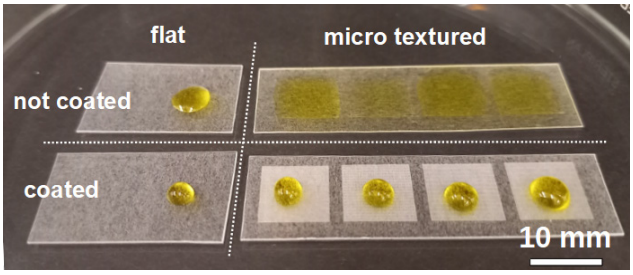

Fig. 4 Linseed oil droplets deposited on hot embossed PMMA without and with applied Mecasurf coating on flat (left) and micro-textured (right) PMMA.

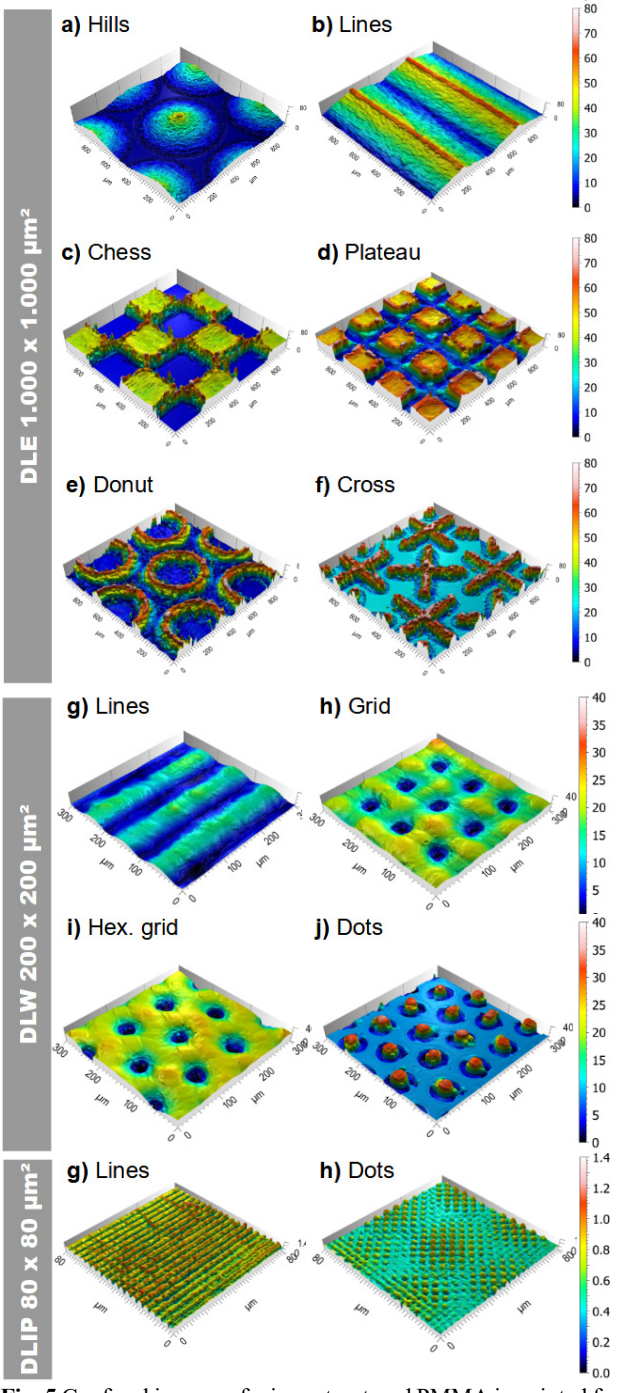

Fig. 5 Confocal images of micro-structured PMMA imprinted from laser textured stamps using (a-f) DLE, (g-j) DLW and (k-l) DLIP technique. Structure periods were a,b,e,f) 500 µm, c,d) 300 µm, (g-j) 80 µm and (k-l) 4.3 µm.

3.2 Wetting behavior of PMMA foils with complex structure geometry

The results reported in section 3.1 permitted to find convenient laser and embossing parameters for producing simple geometries. However, other topographies might be relevant for controlling the wettability of oils and water on PMMA foils. Therefore, in this section, we focus on the fabrication and replication of complex structures, following the parameters already reported. In this section, only confocal images of micro-structured PMMA are shown.

DLE structures in Figure 5a-f were processed with 40 scans and structure periods from 300 µm to 900 µm. Different geometries were produced, namely hills, lines, chess-like, cross-like, donut-like and grid-like patterns. Confocal measurements revealed that for all geometries, structure heights of 45 – 75 µm were achieved (similarly to the results obtained from simple geometries). On geometries with sharp edges, such as chess- or plateau-like structures, the contours showed a lower homogeneity, which is a result of laser processing with ns-pulses at high depths. Within the last layers of engraving, an important amount of energy is concentrated in small areas, leading to partly higher ablation and movement of molten material. This formed random grooves on the master that became bulky material formations on the imprints.

Smaller structures were achieved using the DLW techniques to create line-like structures and dot-like textures, as shown in Figure 5g-j. For line-like textures, the metal surface was scanned 20 times with a pulse duration 30 ns and a fluence of 9.9 J/cm², resulting in smooth grooves with depths of 14 µm. On the imprint, each processed line forms a ridge-like structure with heights up to 14 µm. The grid-like and hexagonal-grid-like structures in Figure 5h-i were processed by repeating the scanning two times with a shift of 90° and three times with a shift of 60°, respectively. As a result, pits were created on the polymer with cross-like or hexagonal arrangement. The size of the pits was controlled by increasing the line-to-line width. The depth of the pits was 16 µm for crossed lines and 26 µm for hexagonal lines.

The dot-like texture in Figure 5j was created by structuring the stamp with 40 pulses at single positions with a spot-to-spot distance of 80 µm. Each hole in the master led to a pillar-like structure on the imprint with a maximum height up to 26 µm on the imprint. Each pillar is surrounded by a round grove with a depth of 5 µm, which is a replication of molten material around the laser drilled holes in the metal master.

The smallest structure resolution was achieved with two- and four-beam DLIP, as depicted in Figure 5g-h. For two-beam DLIP, the incident angle of the sub beams was set to 18°, which resulted in a structure period of 3.4 µm for the used wavelength (note that the period in Figure 1c was 4.3 µm). An overlap of 90 % was used to achieve structure depths of up to 0.7 µm.

The dot-like DLIP structures, shown in Figure 5h was processed with four beams with an incident angle of 12.7°. Ten pulses were applied to each position with a spot-to-spot distance of 40 µm. The period measured in this case was 4.3 µm. The height of the structures was 512 nm (at the center of the interference spot). The height drops with increasing distance from the center, which can be attributed to the Gaussian intensity distribution of the used laser source. Additional stamps were fabricated by DLIP with period in the range between 1.5 µm and 4.5 µm.

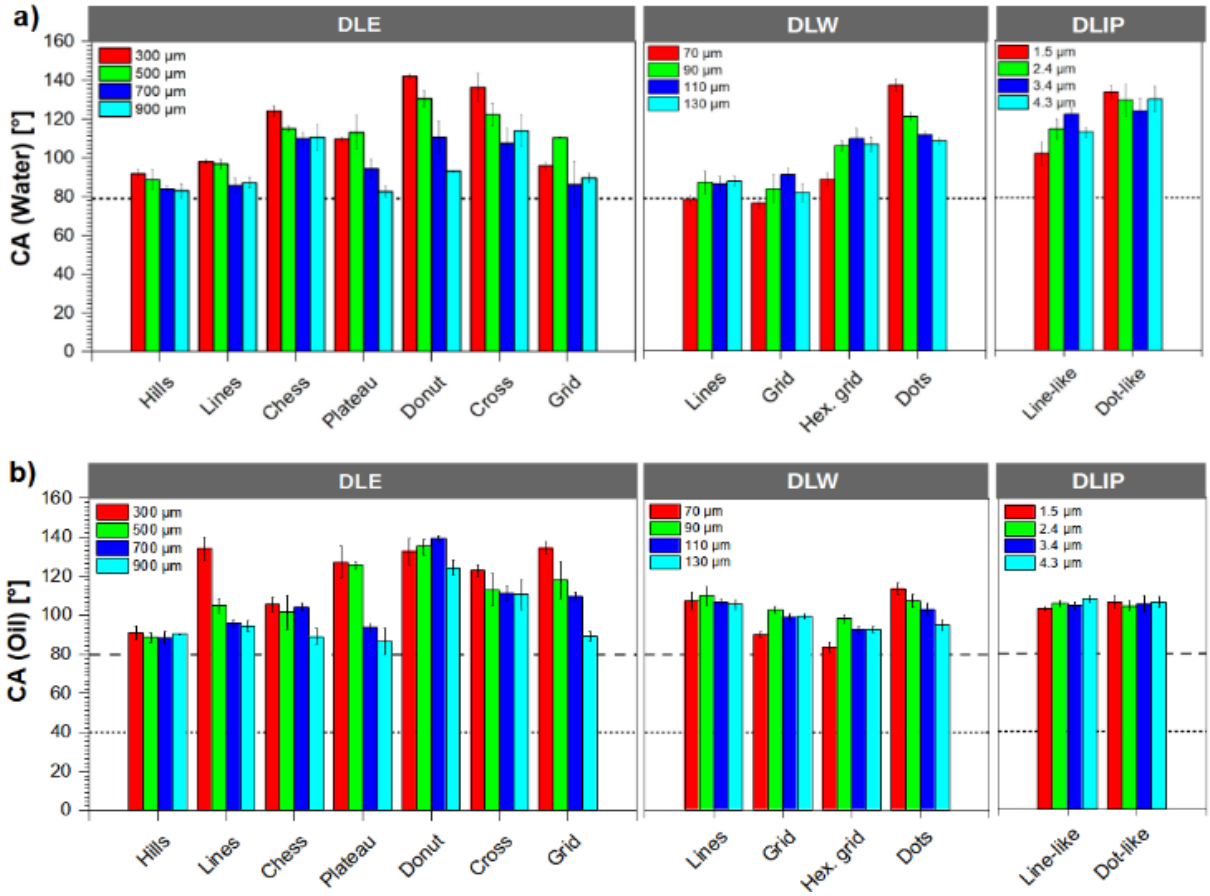

Fig. 6 Static contact angles for (a) deionized water and (b) linseed oil on micro structured PMMA for various structure geometries. Dashed lines represent the references, where 79° for water, and 81° for oil with Mecasurf coating were determined.

Contact angle (CA) measurements were also performed, for the above described structures. As shown in section 3.1, the desired oleophobic behavior could only be achieved for chemically modified surfaces. Therefore, the samples with complex geometries were coated with Mecasurf before the CA measurements. For each measurement, five droplets of either water or oil, with a volume of 4 µl were carefully placed on the micro-textured PMMA imprints.

The results of the water CA measurements are summarized in Figure 6a. Several trends can be observed. For all surface geometries, an increase in CA was found in comparison to the flat reference (dotted line). Depending on the structure geometry and period, the wetting behavior changed from hydrophilic to hydrophobic. For DLE structures, a decrease in the structure period led to an increase in CA. In addition, the structure geometry had also a significant influence on the wetting. Wall- or column-like elevations achieved higher contact angles than flat structure types. The effects were particularly visible with donut-like structures; in this case the contact angle increased from 93° at a period of 900 µm to 142° at a period of 300 µm.

For DLW, a significant increase was obtained for column-like structures (DLW dots) from 94° to 113°, with the CA increasing with shorter distances between the columns. DLIP dot structures showed increased hydrophobic behavior compared to line-like ones, with no significant difference between structure periods (~ 129 °).

As already discussed in section 3.1, the results of the water contact angle measurements suggest a wetting condition described by Cassie-Baxter's theory. The droplets rest on the highest points of the surface and an air barrier is formed between liquid and surface. Higher angles were achieved with increasing density of contact points.

The oil contact angles on the coated surfaces are shown in Figure 6b. Again, an increase in the contact angle was observed with smaller structure periods. For example, a DLE cross-structure with a period of 900 µm showed a contact angle of 89°, which is only a small increase compared to the unstructured reference with 81°. For a period of 300 µm, a contact angle of 136° was measured.

For line-like DLE structures, a maximum value of 134° was found at a period of 300 µm. For this geometry, the measurements were performed in the direction parallel to the lines. Also, a deformation of the droplets in the direction of the structure was observed (not shown). It can be assumed that the wall-like structures impede the flow of oil at small periods orthogonal to the structure direction.

In DLW, pillar-like structures with a spacing of 70 µm showed the highest contact angle of 114°. With increasing distance between the columns, the CA drops to 103° at 130 µm. For line structures, simple lines show higher contact angles than cross or hexagonal-cross structures, although no significant difference was observed between the structure periods.

DLIP structures showed an increase in oil contact angle to an average of 105°, but no significant effect depending on both structure period or geometry was observed.

3.3 Wetting behavior of hierarchical structures

Following the results of the preliminary tests, different surface geometries were combined. For instance, the DLE grid-like pattern (Figure 1a), DLE donut-like pattern (Figure 5e) and the DLW dot-like pattern (Figure 5j) were selected for the fabrication of a hierarchical surface because of the high CA angles achieved for both water and oil.

Figure 7a show a steel surface which was structured first with a DLE grid-like pattern with a period of 500 µm and then with a DLW dot-like pattern with a period of 60 µm. The process parameters corresponded to those of the preliminary tests. The cross-like trenches with a width of 90 µm are the result of the DLE structuring. For the DLE pattern, structure depths of 71 µm were measured.

Ring-hole-like depressions with a diameter of 50 µm can be seen on the entire steel surface as a result of DLW processing (Figure 7a and 7b). The dot-like structures showed depths of 8.9 µm on average. Surprisingly, the DLW textures were 14 µm less deep than on the surfaces of the preliminary tests. This could be due to a change in the melt pool dynamics. The holes of the ns-laser process are mainly formed by the expulsion of melt from the hottest areas in the center of the laser spot. The melt moves up the hole edges by Marangoni convection, resulting in the characteristic accumulations of material around the hole. However, previous DLE machining roughens the surface and disturbs the heat flow near the deep engravings. As a result, the melt movement of the subsequent DLW machining is impeded and more material remains in the machining zone. This behavior is well known and described in detail elsewhere [43-45].

Figure 7c show an imprint on PMMA produced with the steel master with DLE grid-like structure and DLW dot-like structure. As it can be seen, both DLE structures (wall-like elevation) and DLW structures (pillars) were transferred to the polymer over a large area. The wall structures showed a height of 69 µm and the pillars a height of 8.7 µm. Comparable imprint structures were also obtained for a combination of DLE donut and DLW dots, as shown in Figure 7d.

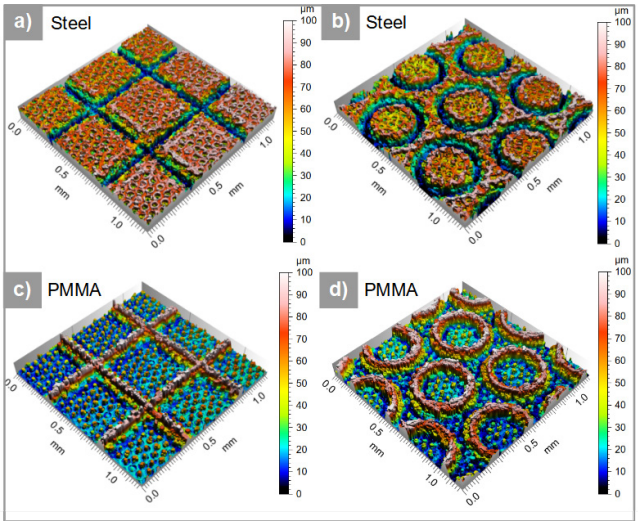

Fig. 7 Stainless steel master (a,b) and corresponding PMMA imprint (c,d) for texture combinations of a DLW dot-like texture with a period of 60 µm and DLE textures with a period of 500 µm with (a) grid and (b) donut geometry.

The hierarchical surfaces were also characterized regarding their wetting behavior. Figure 8 shows the measured water contact angles for water and linseed oil droplets for hierarchically hot embossed PMMA film. The DLW structure period was set constant at 60 µm while the structure period

of the DLE structure was varied between 300 - 900 µm. The drop volume was 4 µl for both liquids. As before, the surfaces for the oil tests were previously coated with Mecasurf. Without the coating, the surfaces showed super-oleophilic behavior with contact angles below 5°.

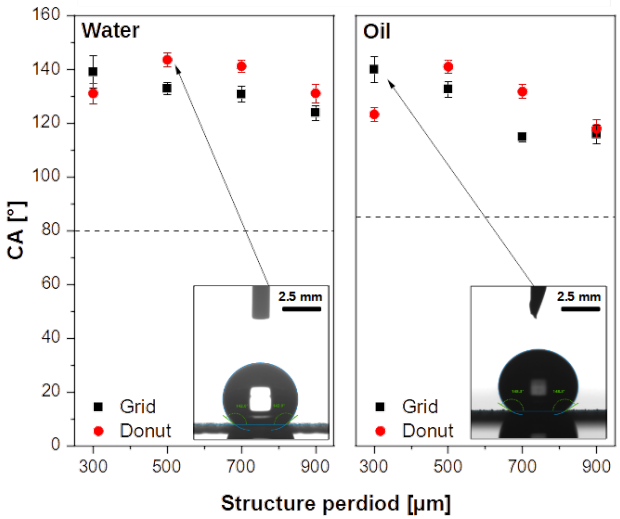

Fig. 8 Static contact angle for 4 µl sized water and linseed oil droplets on hierarchical micro-structured and coated PMMA for DLE structure periods between 300 µm – 900 µm. Dashed lines indicates reference on unstructured surfaces.

Reference measurements on a flat surface are shown as dashed lines. It can be clearly seen that all fabricated structures exhibited higher CA than the unstructured references. The highest contact angles of 144° for water and 141° for oil were determined for a donut structure with a period of 500 µm. Thus, the contact angle for both liquids was increased by about 7° compared to single-scale donut structures. With respect to DLW point structures of comparable height, the increase was of 37° for water and 28° for the linseed oil.

During the wetting experiments, it was observed that water and oil droplets did not detach from the structured surfaces even at high tilting angles. For instance, Figure 9 shows droplets of linseed oil with a size of 8 µl on a hot embossed PMMA film with four hierarchically micro-structured surfaces with varying period (see labels in Figure 9) when rotated by 180°. It can be clearly seen that the droplets do not detach from the surface despite high wetting angles. This effect, also known as the rose-petal effect, has already been observed for water on PMMA [46].

For up-scaling the presented approach, the processed areas and throughputs must be compatible with industrial applications. Thanks to the availability of high-power and high-frequency lasers, surface structures can be patterned at high scanning velocities and over large areas using galvanometer scanners or polygon scanners, whereby DLIP throughputs of 1.1 m²/min have already been reported [47]. For the hot embossing step, plate-to-roll or roll-to-roll strategies can be adopted. Recently, a roll-to-roll hot embossing unit equipped with DLIP-processed cylindrical molds was employed to achieve web speeds of 50 m/min [48].

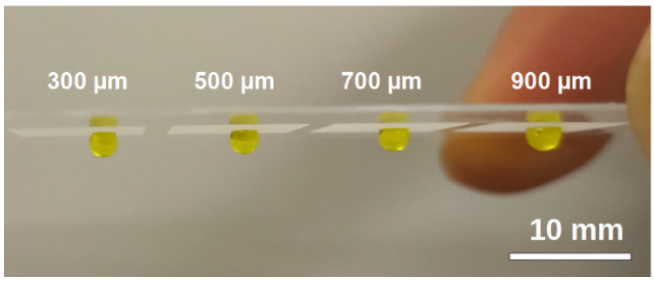

Fig. 9 Sticking linseed oil droplets with a volume of 8 µl on a micro-textured PMMA foil with a hierarchical grid-like texture with various structure periods.

4. Conclusions

In this study, micro-structured PMMA surfaces were investigated with regard to their wetting behavior with polar and nonpolar liquids for easy-to-clean applications. The micro-structures were first produced on stainless steel using the laser-based processes DLE, DLW and DLIP with feature sizes from 1.5 µm to 900 µm and then transferred to PMMA foils using plate-to-plate hot embossing. Confocal examination revealed sufficient transfer quality with texture heights from 0.09 µm to 85.0 µm.

Contact angle measurements were performed with deionized water and linseed oil. It could be shown that the structure depth, period and shape strongly affects the wetting behavior. Water contact angles up to 142° have been measured on DLE structures with donut shape and a period of 300 µm. For oil, a nearly super-oleophilic state with contact angle of 5.3° was found on a DLIP line-like texture with a period of 3.4 µm. The effects of coating with a hydrophobic agent (Mecasurf) was also investigated. While no change occurred for water, the surfaces changed to a strongly oleophobic condition with contact angles up to 140°.

Finally, hierarchical surfaces were produced by combining DLE and DLW structuring. It was shown that the combination of structures increased the contact angles for water to 142° and for oil (coated surface) to 141°C. This corresponds to an increase of 7° compared to the corresponding single-scale structures. The polymer film processed in this way could be of interest for easy-to-clean applications in displays, sensors or in architecture.

Acknowledgments

The work of F.B. was performed in the framework of the Reinhart–Koselleck project (323477257), which has received funding from the German Research Foundation (German: *Deutsche Forschungsgemeinschaft DFG*). M.S. and W.W. acknowledge the German Federal Ministry of Education and Research (BMBF) for financial support, under the program WIR – GRAVOMER, project “03WIR2003B”.

References

[1] T. Darmanin and F. Guittard: Mater. Today, 18, (2015) 273.
[2] T. B. H. Schroeder, J. Houghtaling, B. D. Wilts, and M. Mayer: Adv. Mater., 30, (2018) 1705322.
[3] A. Y. Vorobyev and C. Guo: J. Appl. Phys., 117, (2015) 033103.
[4] Y. Y. Yan, N. Gao, and W. Barthlott: Adv. Colloid Interface Sci., 169, (2011) 80.

[5] M. V. Kahraman, Z. S. Akdemir, İ. Kartal, N. Kayaman-Apohan, and A. Güngör: Polym. Adv. Technol., 22, (2011) 981.
[6] I. Yilgor, S. Bilgin, M. Isik, and E. Yilgor: Polymer, 53, (2012) 1180.
[7] D. Ebert and B. Bhushan: Langmuir, 28, (2012) 11391.
[8] D. Korzec, F. Hoppenthaler, T. Andres, S. Guentner, and S. Lerach: Plasma, 5, (2022) 111.
[9] N. Vourdas, A. Tserepi, and E. Gogolides: Nanotechnology, 18, (2007) 125304.
[10] E. K. Her, T.-J. Ko, B. Shin, H. Roh, W. Dai, W. K. Seong, H.-Y. Kim, K.-R. Lee, K. H. Oh, and M.-W. Moon: Plasma Processes Polym., 10, (2013) 481.
[11] H. W. Choi, S. Bong, D. F. Farson, C. Lu, and L. J. Lee: J. Laser Appl., 21, (2009) 196.
[12] C. De Marco, S. M. Eaton, R. Suriano, S. Turri, M. Levi, R. Ramponi, G. Cerullo, and R. Osellame: ACS Appl. Mater. Interfaces, 2, (2010) 2377.
[13] J. Hildenhagen, K. Dickmann, J. Neyer, and C. Wieschendorf: Proc. SPIE, (2013), p. 87691D.
[14] K. Ellinas, A. Tserepi, and E. Gogolides: Langmuir, 27, (2011) 3960.
[15] S. S. Deshmukh and A. Goswami: Mater. Manuf, 36, (2021) 501.
[16] S. S. Deshmukh and A. Goswami: IOP Conf. Ser.: Mater. Sci. Eng., 872, (2020) 012069.
[17] J. A. Gomez, G. T. Conner, D. H. Chun, Y.-J. Kim, I.-H. Song, and B. H. You: Fibers Polym., 15, (2014) 1197.
[18] M. Röhrig, M. Schneider, G. Etienne, F. Oulhadj, F. Pfannes, A. Kolew, M. Worgull, and H. Hölscher: J. Micromech. Microeng., 23, (2013) 105014.
[19] G. Fu, S. B. Tor, N. H. Loh, and D. E. Hardt: Appl. Phys. A, 97, (2009) 925.
[20] J. Zhu, Y. Tian, C. Yang, L. Cui, F. Wang, D. Zhang, and X. Liu: Microsyst. Technol., 23, (2017) 5653.
[21] K. Ahmmed, C. Grambow, and A.-M. Kietzig: Micromachines, 5, (2014) 1219.
[22] X. Wang and H. Zheng: J. Laser Appl., 30, (2018) 032203.
[23] L. Mulko, M. Soldera, and A. F. Lasagni: Nanophotonics, 11, (2022) 203.
[24] V. Furlan, M. Biondi, A. G. Demir, B. Previtali, G. Pariani, and A. Bianco: J. Vac. Sci. Technol. B, 36, (2018) 01A102.
[25] P. Hauschwitz, D. Jochcová, R. Jagdheesh, D. Rostohar, J. Brajer, J. Kopeček, M. Cimrman, M. Smrž, T. Mocek, and A. Lucianetti: Opt, 133, (2021) 106532.
[26] J. Bonse and S. Gräf: Laser Photon. Rev., 14, (2020) 2000215.
[27] S. Gräf: Adv, Opt. Technol., 9, (2020) 11.
[28] T.-F. Yao, P.-H. Wu, T.-M. Wu, C.-W. Cheng, and S.-Y. Yang: Microelectron. Eng., 88, (2011) 2908.
[29] J.-H. Rakebrandt, Y. Zheng, H. Besser, T. Scharnweber, H. J. Seifert, and W. Pfleging: Microsyst. Technol., 26, (2020) 1085.
[30] J. T. Cardoso, A. I. Aguilar-Morales, S. Alamri, D. Huerta-Murillo, F. Cordovilla, A. F. Lasagni, and J. L. Ocaña: Opt. Lasers Eng., 111, (2018) 193.
[31] F. Bouchard, M. Soldera, R. Baumann, and A. F. Lasagni: Materials, 14, (2021) 1756.
[32] C. H. Wu, C. H. Hung, and Y. Z. Hu: AMR, 74, (2009) 251.
[33] E. Nikolidakis, I. Choreftakis, and A. Antoniadis: Machines, 6, (2018) 40.
[34] T.-N. Le and Y.-L. Lo: Mater. Design, 179, (2019) 107866.
[35] T. Fuhrich, P. Berger, and H. Hügel: J. Laser Appl., 13, (2001) 178.
[36] T. Knebel, A. Streek, and H. Exner: Phys. Procedia, 56, (2014) 19–28.
[37] M. M. Pariona, A. F. Taques, and L. A. Woiciechowski: Inter. J. Heat Mass Transf., 119, (2018) 10.
[38] N. Encinas, M. Pantoja, J. Abenojar, and M. A. Martínez: J. Adh. Sci. Technol., 24, (2010) 1869.
[39] M. Kanungo, S. Mettu, K.-Y. Law, and S. Daniel: Langmuir, 30, (2014) 7358.
[40] R. N. Wenzel: Ind. Eng. Chem., 28, (1936) 988.
[41] A. B. D. Cassie and S. Baxter: Trans. Faraday Soc., 40, (1944) 546.
[42] A. I. Aguilar-Morales, S. Alamri, B. Voisiat, T. Kunze, and A. F. Lasagni: Materials, 12, (2019) 2737.
[43] Q. Guo, C. Zhao, M. Qu, L. Xiong, S. M. H. Hojjatzadeh, L. I. Escano, N. D. Parab, K. Fezzaa, T. Sun, and L. Chen: Addit. Manuf., 31, (2020) 100939.
[44] T. Fuhrich, P. Berger, and H. Hügel: J. Laser Appl., 13, (2001) 178.
[45] K.-H. Leitz, B. Redlingshöfer, Y. Reg, A. Otto, and M. Schmidt: Phys. Procedia, 12, (2011) 230.
[46] C. Wang, R. Shao, G. Wang, and S. Sun: Colloids Surf., 622, (2021) 126661.
[47] F. Ränke, R. Baumann, B. Voisiat, and A. Fabián Lasagni: Materials Lett. X, 14, (2022) 100144.
[48] A. Rank, V. Lang, and A. F. Lasagni: Adv. Eng. Mater., 19, (2017) 1700201.

(Received: May 30, 2022, Accepted: September 2, 2022)